THE JOURNAL OF BIOLOGICAL CHEMISTRY VOL. 284, NO. 38, pp. 26117–26126, September 18, 2009

Evidence for the Direct Interaction of Spermine with the Inwardly Rectifying Potassium Channel*[S]

Received for publication, June 5, 2009 Published, JBC Papers in Press, July 20, 2009, DOI 10.1074/jbc.M109.029355

Masanori Osawa[‡], Mariko Yokogawa[‡1], Takahiro Muramatsu[‡], Tomomi Kimura[‡], Yoko Mase[‡], and Ichio Shimada[‡§2]

From the [‡]Division of Physical Chemistry, Graduate School of Pharmaceutical Sciences, The University of Tokyo, Hongo, Bunkyo-ku, Tokyo 113-0033, Japan and the [§]Biomedicinal Information Research Center (BIRC), National Institute of Advanced Industrial Science and Technology (AIST), Aomi, Koto-ku, Tokyo 135-0064, Japan

The inwardly rectifying potassium channel (Kir) regulates resting membrane potential, K^+ homeostasis, heart rate, and hormone secretion. The outward current is blocked in a voltage-dependent manner, upon the binding of intracellular polyamines or Mg^{2+} to the transmembrane pore domain. Meanwhile, electrophysiological studies have shown that mutations of several acidic residues in the intracellular regions affected the inward rectification. Although these acidic residues are assumed to bind polyamines, the functional role of the binding of polyamines and Mg^{2+} to the intracellular regions of Kirs remains unclear. Here, we report thermodynamic and structural studies of the interaction between polyamines and the cytoplasmic pore of mouse Kir3.1/GIRK1, which is gated by binding of G-protein $\beta\gamma$-subunit ($G\beta\gamma$). ITC analyses showed that two spermine molecules bind to a tetramer of Kir3.1/GIRK1 with a dissociation constant of 26 μM, which is lower than other blockers. NMR analyses revealed that the spermine binding site is Asp-260 and its surrounding area. Small but significant chemical shift perturbations upon spermine binding were observed in the subunit-subunit interface of the tetramer, suggesting that spermine binding alters the relative orientations of the four subunits. Our ITC and NMR results postulated a spermine binding mode, where one spermine molecule bridges two Asp-260 side chains from adjacent subunits, with rearrangement of the subunit orientations. This suggests the functional roles of spermine binding to the cytoplasmic pore: stabilization of the resting state conformation of the channel, and instant translocation to the transmembrane pore upon activation through the $G\beta\gamma$-induced conformational rearrangement.

The inwardly rectifying K^+ channel (Kir)[3] plays a pivotal role in controlling resting membrane potential, K^+ homeostasis, heart rate, and hormone secretion (1). The inward rectification property of Kir is reportedly due to the voltage-dependent blockade of the outward current by intracellular polyamines and Mg^{2+} (2–6). The importance of the electrostatic interactions of polyamines and Mg^{2+} with the acidic residues in Kirs has been indicated by electrophysiological studies in combination with site-directed mutagenesis, which have been accelerated by the recent progress in the structural analyses of Kirs (7–10). The crystal structures revealed that they form a symmetric tetramer, in which the transmembrane pore, containing the K^+-selective filter and the cytoplasmic pore consisting of the N- and C-terminal regions form a long pore for the K^+ pathway.

In Kir2.1/IRK1, the strongest inward rectifier in the Kir family, negatively charged acidic residues that influence the inward rectification have been identified, including Asp-172 (11) in the transmembrane pore and Glu-224, Asp-255, Asp-259, and Glu-299 in the cytoplasmic pore (9, 12–19). These acidic residues are assumed to be responsible for the electrostatic interaction with polyamines, in which the nitrogen atoms are positively charged at neutral pH (20).

In other members of the Kir family, some of the electronegative residues are replaced by neutral ones, such as Gly and Ser. Although the total number of acidic residues correlates with the strength of inward rectification, the correlation cannot be completely explained for the strong rectifiers (9). In Kir3.1/GIRK1, which exhibits relatively strong inward rectification among the Kir family proteins, two of the four important acidic residues in Kir2.1 (Glu-224 and Asp-255) are replaced by Ser (Ser-225 and Ser-256 in Kir3.1, respectively). This suggests that the binding site(s) and stoichiometry of polyamine binding differ among the Kir proteins.

Although the binding of polyamines to the cytoplasmic pore of Kirs is considered to be required for the blockade of the transmembrane pore to enable the inward rectification (16, 19, 21), the functional role of the polyamine binding to the cytoplasmic pore is still unclear. In particular, Kir3/GIRK is activated by the binding of G-protein $\beta\gamma$-subunits ($G\beta\gamma$) to the cytoplasmic pore through the conformational rearrangement of the channel (22). Thus, the elucidation of the binding mode of Kir and polyamines based on the detection of their direct interaction as well as the effects of the binding on the protein conformation provides insights into the functional roles of the cytoplasmic pore in the gating and the inward rectifying property of the channel.

Here, we report the thermodynamic and structural analyses of the interaction between spermine and the intracellular

* This work was supported in part by grants from the Japan New Energy and Industrial Technology Development Organization (NEDO) and the Ministry of Economy, Trade, and Industry (METI) (to I. S.), a grant-in-aid for Scientific Research on Priority Areas from the Japanese Ministry of Education, Culture, Sports, Science, and Technology (to M. O. and I. S.), and a grant from Takeda Science Foundation (to M. O.).

[S] The on-line version of this article (available at http://www.jbc.org) contains supplemental Figs. S1 and S2.

[1] A research fellow of the Japan Society for the Promotion of Science (JSPS).

[2] To whom correspondence should be addressed: 7-3-1 Hongo, Bunkyo-ku, Tokyo 113-0033, Japan. Tel. and Fax: 81-3-3815-6540; E-mail: shimada@iw-nmr.f.u-tokyo.ac.jp.

[3] The abbreviations used are: Kir, inwardly rectifying potassium channel; $G\beta\gamma$, G-protein $\beta\gamma$-subunit; GIRK, G-protein gated inwardly rectifying potassium channel; $GIRK_{CP}$, cytoplasmic pore domain of GIRK; ITC, isothermal titration calorimetry; CSP, chemical shift perturbation; PDB, Protein Data Bank.

regions of Kir3.1/GIRK1. Our isothermal titration calorimetry (ITC) results indicated that two spermine molecules bind to a tetramer of Kir3.1/GIRK1, with a dissociation constant (K_d) value of 26 μM. NMR analyses together with ITC results revealed the spermine binding mode, in which one spermine molecule bridges two Asp-260 side chains of two adjacent subunits, with the alteration of the relative orientations of the four subunits. The spermine binding mode revealed here suggests the functional roles of the spermine binding to the cytoplasmic pore: in the resting state of the channel, spermine stabilizes a certain channel conformation, and upon activation, spermine is dissociated from the cytoplasmic pore through the G$\beta\gamma$-induced conformational rearrangement, leading to rapid translocation to the transmembrane pore to block the outward K^+ current.

EXPERIMENTAL PROCEDURES

Sample Preparation—The N- and C-terminal intracellular regions (residues 41–63 and 190–371) of mouse Kir3.1/GIRK1 were fused into a single polypeptide, which is hereafter referred to as $GIRK_{CP}$ (cytoplasmic pore). The sample preparation of $GIRK_{CP}$ is described elsewhere (23). Briefly, the DNA encoding $GIRK_{CP}$ with ten N-terminal His residues, followed by the PreScission protease cleavage site, was inserted into the pET24d(+) plasmid, which was transformed into the *Escherichia coli* C41 strain. Mutations were introduced by the QuikChange® (Stratagene) method. $GIRK_{CP}$ and its mutants were overexpressed in the C41 strain and were purified to homogeneity by His-select Ni affinity chromatography, His tag cleavage by PreScission protease, and then gel filtration using Superdex 200 PG (GE Healthcare). The elution profile of the gel-filtration column indicated that $GIRK_{CP}$ forms a tetramer, which was confirmed by a calibration curve made by standard proteins for molecular mass as well as the SEC-MALS experiments (see supplemental Fig. S1 for details). We prepared uniformly ^2H,^{15}N-labeled $GIRK_{CP}$, whose amide hydrogen atoms were fully exchanged to ^1H by unfolding with 6 M guanidine and subsequent refolding.

Isothermal Titration Calorimetry (ITC)—The binding of spermine and Mg^{2+} to $GIRK_{CP}$ and its mutants was measured by ITC (24), using a MicroCal VP-ITC MicroCalorimeter (MicroCal Inc.). The protein samples were dialyzed against a buffer containing 10 mM HEPES·NaOH (pH 7.0), 0–150 mM KCl, and 5 mM dithiothreitol. 900 μM spermine and 1.4 mM $MgCl_2$ in the dialysis buffer were prepared as the injection solutions. Experiments were performed at 15–30 °C. A 30–47 μM solution of $GIRK_{CP}$ tetramer or its mutants was titrated by the injection of a total of 290 μl of 900 μM spermine or 1.4 mM $MgCl_2$ in 29 aliquots. Because essentially no heat of dilution was observed by titrating the spermine solution into the dialysis buffer, the raw titration data were analyzed using the MicroCal Origin software version 5.0, provided by the manufacturer. The heat of dilution of $MgCl_2$ was subtracted from the data for the $MgCl_2$ titration into $GIRK_{CP}$. The thermodynamic parameters are listed in Tables 1 and 2.

NMR Analyses—All NMR experiments were performed at 35 °C on a Bruker Avance-800 or Avance-600 spectrometers equipped with cryogenic probes. The sample concentrations of $GIRK_{CP}$ and its mutants were 100–200 μM as the tetramer.

To observe intermolecular NOE signals between spermine and $GIRK_{CP}$, ^{15}N-edited NOESY HSQC spectra were observed for uniformly ^2H,^{15}N-labeled $GIRK_{CP}$, and the mutants Q271A, Q261A, and Q227A/Q261A, in 50 mM HEPES·NaOH buffer (pH 7.0), containing 50 mM KCl, 5 mM dithiothreitol, and 8%(v/v) D_2O. A two-dimensional NOESY spectrum was observed for the uniformly ^2H-labeled $GIRK_{CP}$, in which only isoleucine, methionine, or phenylalanine residues were selectively ^1H,^{15}N-labeled. The F255A mutant was also phenylalanine-selectively ^1H,^{15}N-labeled in a ^2H-background, to confirm the assignments of the intermolecular NOE signals between Phe-255 and spermine. Each sample contained spermine at a 5 equiv. amount relative to the protein. The NOE mixing time was set at 300 ms.

An aliquot of 700 μM spermine solution dissolved in the NMR sample buffer was used for the titration experiments, in which 0.25, 0.50, 0.75, 1.0, 2.0, 3.0, 4.0, and 5.0 equivalents of a tetramer of uniformly ^2H,^{15}N-labeled $GIRK_{CP}$ was added. After the addition of each aliquot of spermine, one-dimensional ^1H and two-dimensional ^1H-^{15}N TROSY spectra were acquired. The titration was performed up to a maximum spermine:tetramer of $GIRK_{CP}$ molar ratio of 5:1. It should be noted that $GIRK_{CP}$ exhibits no chemical shift change at the concentration range from 20 to 300 μM as a tetramer, and thus, the chemical shift changes through the spermine titration is not due to the sample dilution but the effects arisen from the interaction with spermine. The assignments of the backbone NMR signals from $GIRK_{CP}$ were reported (BioMagResBank accession number: 11067 (23)). The assignments for the spermine-bound form of $GIRK_{CP}$ were transferred from those in the absence of spermine by tracing the chemical shift perturbation (CSP) upon spermine addition. The assignments for the spermine-bound form were confirmed by ^{15}N-edited NOESY TROSY of the partially protonated $GIRK_{CP}$, which was expressed in D_2O-based M9 medium containing 1 g/liter ^1H-glucose. The normalized CSP values ($\Delta\delta$) were obtained using the formula, $\Delta\delta = \{(\Delta\delta_{1H})^2+(\Delta\delta_{15N}/6.5)^2\}^{0.5}$ (25). The error values were calculated by the formula, $2\cdot(\Delta\delta_{1H}\cdot R_{1H} + \Delta\delta_{15N}\cdot R_{15N}/6.5^2)/\Delta\delta$, where R_{1H} and R_{15N} are the digital resolutions in ppm in the ^1H and ^{15}N dimensions, respectively.

^1H-^{15}N TROSY spectra were observed for the E250N, D260N, D275N, and E300N mutants, and were compared with the spectrum of $GIRK_{CP}$, to ascertain the structural effects of the mutations.

RESULTS

Two Spermine Molecules Bind to the Intracellular Regions of Kir3.1/GIRK1—In this study, we used the cytoplasmic pore of mouse Kir3.1/GIRK1, referred to as $GIRK_{CP}$, which consists of residues 41–63 and 190–371 as a single polypeptide. The validity of this construct was indicated by its crystal structure (7, 9), which was essentially identical to the structures of the cytoplasmic pores in the full-length Kir channels, such as KirBac1.1 and a chimera of KirBac1.3 and Kir3.1 (8, 10). $GIRK_{CP}$ was expressed in *E. coli*, and was purified to homogeneity. Size exclusion chromatography analyses in combination with mul-

tiple-angle light scattering (SEC-MALS) indicated that the average molecular mass was 92 K (supplemental Fig. S1), corresponding to a tetramer of the theoretical mass of 24 K protein.

ITC experiments were carried out to compare the binding properties of $GIRK_{CP}$ with spermine, spermidine, putrescine, and Mg^{2+}. Fig. 1*A* shows the isotherms upon the titration of spermine into the $GIRK_{CP}$ solution. The best fit of the integrated isotherms using a single-site model indicated that two spermine molecules bind to a $GIRK_{CP}$ tetramer with a dissociation constant (K_d) value of 500 nM, in 50 mM KCl at 303 K. Spermidine and Mg^{2+} exhibited significantly lower affinities to $GIRK_{CP}$ (Fig. 1*B* and Table 1), which was 30- and 120-fold lower than spermine, respectively. A titration curve was not obtained for putrescine, although a certain amount of heat exchange was observed, suggesting that the binding is weak ($K_d > 1$ mM). Because the intracellular concentrations of spermine and spermidine are 0.1–1.0 mM, and 1.0–10 mM for Mg^{2+}, spermine is the major binder to the intracellular regions of Kir3.1/GIRK. Therefore, our further analyses were focused on spermine as a Kir blocker.

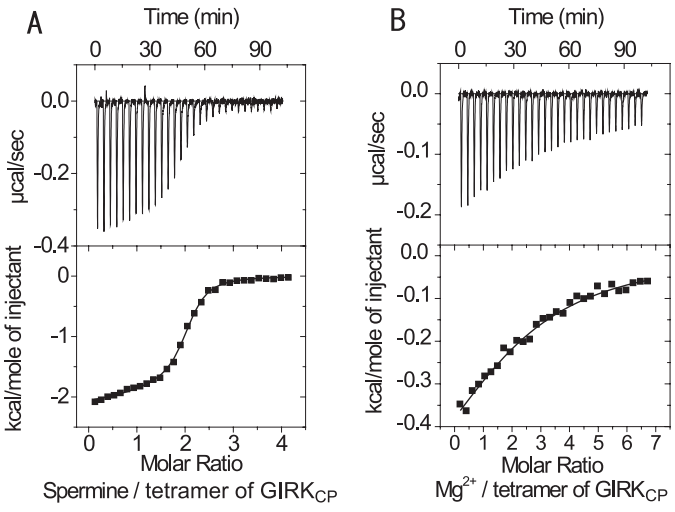

FIGURE 1. **Isothermal titration microcalorimetric analyses of the interactions between $GIRK_{CP}$ and spermine or $MgCl_2$.** *Upper panel*, trace of the calorimetric titration of 29 × 10 μl aliquots of spermine (*A*) and $MgCl_2$ (*B*) into the cell containing $GIRK_{cp}$. *Lower panel*, integrated binding isotherm obtained from the experiment. *A*, two-site model with the fixed binding stoichiometry of 1 for the binding of the first spermine molecule was applied to fit the data. *B*, single site model was applied to the $MgCl_2$ binding. Parameters obtained from the best fit (*solid line*) are summarized in Table 1.

To estimate the electrostatic contribution to the spermine binding, ITC experiments were performed at various KCl concentrations, from 0 to 150 mM. While the binding stoichiometry was unchanged, the K_d values increased as the KCl concentration increased (Fig. 2 and Table 1). At the nearly physiological KCl concentration of 150 mM, the K_d value was 26 μM.

In addition, the heat capacity change upon binding (ΔC_p), *i.e.* the temperature dependence of the enthalpy change (ΔH), was evaluated by performing the ITC experiment at various temperatures (Fig. 3). At the KCl concentration of 50 mM, ΔC_p was −0.19 kcal/mol K. The negative ΔC_p value suggests that desolvation from the surface of $GIRK_{CP}$ and/or spermine occurs upon binding.

Residues Proximal to Spermine Based on Intermolecular NOEs—The recently reported crystal structure of the cytoplasmic pore of Kir2.1 as well as the site-directed mutagenesis identified four acidic residues (Glu-224, Asp-255, Asp-259, and Glu-299) in the intracellular region that influence inward rectification (9). Two of the corresponding residues are conserved in Kir3.1/GIRK1 (Asp-260 and Glu-300). Although the mutations of these residues impaired the inward rectification in Kir2.1 (9, 13, 14), the residues that directly bind remained unknown. To identify the spermine-interacting residues in Kir3.1/GIRK1, we obtained intermolecular NOEs between $GIRK_{CP}$ and spermine, which in principle are observed between two protons existing within 5 Å.

The proton resonances from spermine were assigned by the combination of NOESY and DQF-COSY experiments. The protons at positions 2 and 6 resonate at 2.1 and 1.7 ppm, respectively, and the signals from positions 1, 3, and 5 are overlapped at 3.1 ppm (Fig. 4*A*). Only one set of NMR signals for spermine was observed. When the spermine concentration was successively increased in the presence of a constant amount of $GIRK_{CP}$, the chemical shift values for the spermine NMR signals gradually shifted up to those in the free-state, indicating that spermine undergoes fast exchange on the NMR time scale between the protein-bound state and the free state. Therefore, we observed the transferred NOE signals as follows, using a sample containing 5 equivalent amount of spermine per $GIRK_{CP}$ tetramer, in which the molar ratio of the bound spermine and free spermine is 2:3.

The ^{15}N-edited NOESY HSQC spectrum for uniformly $^{2}H,^{15}N$-labeled $GIRK_{CP}$ mixed with a saturating amount of spermine exhibited only a few NOE signals between the sperm-

TABLE 1
Thermodynamic parameters for the interaction of $GIRK_{CP}$ with polyamines and $MgCl_2$

Injectant	Temperature	KCl	Model	Stoichiometry per tetramer	K_d	ΔH	ΔS
	K	*mM*			*μM*	*kcal/mol*	*kcal/mol K*
Spermine	303	0	Two sites[a]	First site 1 (fixed)	0.06 ± 0.01	−6.00 (fixed)	0.013
				Second site 0.99 ± 0.01	0.22 ± 0.04	−2.33 ± 0.06	0.23
	303	50	Single sites	1.835 ± 0.007	0.49 ± 0.04	−2.54 ± 0.02	0.020
	303	100	Single sites	1.784 ± 0.007	6.8 ± 0.4	−2.10 ± 0.01	0.017
	303	150	Single sites	1.772 ± 0.004	25.9 ± 0.04	−1.809 ± 0.006	0.015
	283	50	Single sites	1.82 ± 0.01	0.34 ± 0.04	0.839 ± 0.007	0.033
	288	50	Single sites	1.2 ± 0.2	3 ± 3	0.23 ± 0.04	0.026
	293	50	Single sites	1.60 ± 0.01	0.66 ± 0.09	−0.97 ± 0.01	0.025
	298	50	Single sites	1.54 ± 0.01	0.82 ± 0.09	−1.93 ± 0.02	0.021
Spermidine	303	50	Single sites	1.57 ± 0.08	16 ± 3	−2.0 ± 0.1	0.015
Putrescine	303	50	N/A				
$MgCl_2$	298	50	Single sites	2.4 ± 0.2	101 ± 17	−0.7 ± 0.1	0.016

[a] A two-site model was applied, in which the stoichiometry and the ΔH value for the first binding site are fixed as one and the value of the y-section of the isotherm, respectively.

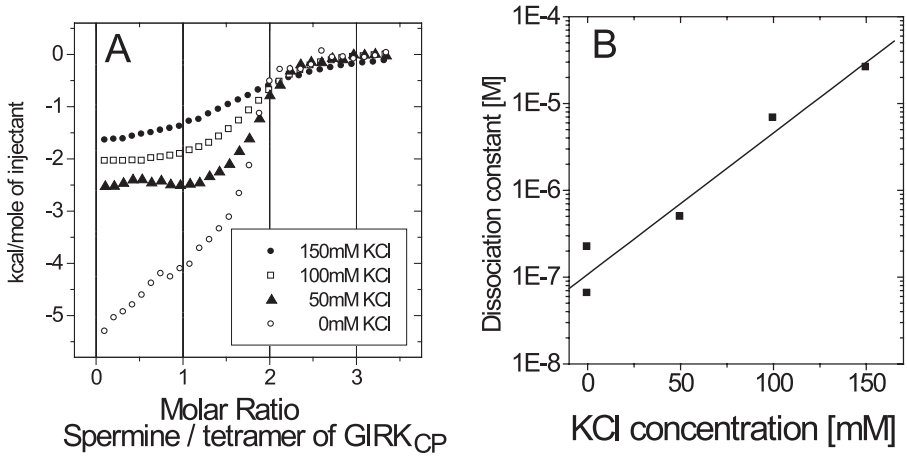

FIGURE 2. **Salt concentration dependence of the GIRK$_{CP}$-spermine interaction.** *A*, binding isotherms at different concentrations of KCl for the GIRK$_{CP}$-spermine interaction. *B*, plot of the dissociation constant value (K_d) against the KCl concentration.

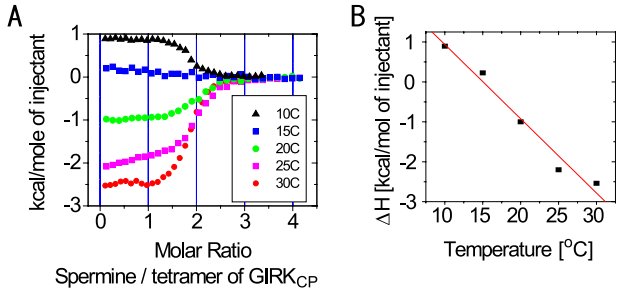

FIGURE 3. **Temperature dependence of the GIRK$_{CP}$-spermine interaction.** *A*, binding isotherms at different temperatures for the GIRK$_{CP}$-spermine interaction. *B*, plot of the enthalpy change (ΔH) against the experimental temperature yielded a ΔC_p value of −0.19 kcal/mol·K as the slope of the fitted line.

ine protons at positions 1/3/5 and 6 and the side chain amide protons of two of the Asn and/or Gln residues (Fig. 4*B*, *black*). The absence of an NOE at position 2 strongly suggests that the NOE signals at 3.1 ppm are probably from position 5, and not from 1 or 3. A closer look at the crystal structure of GIRK$_{CP}$ revealed that there are only two Gln residues (Gln-227 and Gln-261) and no Asn residue among the residues exposed to the cytoplasmic pore. We prepared three mutants (Q227A, Q261A, and Q227A/Q261A), and confirmed their binding affinities for GIRK$_{CP}$ by ITC (Table 2). We then performed ^{15}N-edited NOESY HSQC experiments under the same conditions as those for the wild-type GIRK$_{CP}$. The intermolecular NOE signals for only one Gln residue were observed for the mutants, Q227A and Q261A (supplemental Fig. S2), while no intermolecular NOE signal was observed for the Q227A/Q261A mutant (Fig. 4*B*, *red*). Meanwhile, the ITC experiment indicated that the spermine binding affinity was essentially unchanged by the mutation of Q227A/Q261A (Table 2). Thus, the intermolecular NOEs were assigned between the side chain amide protons of Gln-227 and Gln-261 and the spermine protons at positions 5 and 6. No other NOE signals between the amide protons of the protein and spermine were observed.

Furthermore, we explored the intermolecular NOEs with hydrophobic residues in the vicinity of Gln-227 and Gln-261, which are located between Asp-260 and Glu-300. We prepared the protein samples with Phe, Ile, or Met-selective ^{1}H,^{15}N-labeling in a ^{2}H-background, since Phe-255 and Ile-302 are proximal to Asp-260 and Glu-300, respectively, and Met-308 exists at the exit of the cytoplasmic pore on the membrane side (see Fig. 4*D*). While no intermolecular NOEs were observed for Ile- or Met-selectively ^{1}H-labeled GIRK$_{CP}$, the Phe-selectively labeled protein showed NOE peaks between the aromatic protons of a phenylalanine residue and positions 1/3/5, 2 and 6 of spermine (Fig. 4*C*, *black*). These NOEs were assigned by the fact that the F255A mutant did not exhibit any intermolecular NOEs from the aromatic proton of the mutants (Fig. 4*C*, *red*), while the mutant retained the spermine binding affinity (Table 2).

In summary, Gln-227, Gln-261, and Phe-255 were identified to exist in the proximity (within 5 Å) of the bound spermine molecules. The side chain amide protons of Gln-227 and Gln-261 are close to positions 5 and 6 of the spermine protons, while the aromatic protons of Phe-255 are close to all of the protons of the spermine methylene groups (Fig. 4*D*).

Spermine Binding Induces a Conformational Rearrangement of the Cytoplasmic Pore of Kir3.1/GIRK1—The spermine binding effect on GIRK$_{CP}$ was also investigated by CSP, which reflects the direct spermine-binding as well as the conformational change of the protein. A number of the ^{1}H-^{15}N TROSY signals for the backbone amide groups of GIRK$_{CP}$ changed their chemical shifts upon spermine binding. Fig. 5*A* shows the spectral overlay of the TROSY spectra in the absence and presence of spermine, and a plot of the normalized CSP values ($\Delta\delta$) against the residue numbers of GIRK$_{CP}$. The residues with significant CSPs ($\Delta\delta \geq 0.08$ ppm) are Phe-46, Gly-58, Thr-193, Gln-227, Ser-235, Gln-248, Val-253, Ser-256, Gly-336, and Phe-337 (Fig. 5*B*). The mapping of these residues on the structures (Fig. 5, *panels C* and *D*) indicates that Gln-227, Val-253, and Ser-256 exist at the inner pore site, where the intermolecular NOEs were observed (residues Gln-227, Phe-255, and Gln-261), and that the rest of the perturbed residues are located at the subunit-subunit interface of the tetramer, which is distal to the spermine binding site (Fig. 5*D*). In particular, Phe-46 and Gln-248 form hydrogen bonds with the Glu-294 and Phe-263 of the adjacent subunit, respectively, in the crystal structure of the spermine-free form of the GIRK$_{CP}$ (PDB code: 1N9P). Therefore, the CSPs for the residues at the subunit-subunit interface should be interpreted as the rearrangement of the relative orientations of the subunits.

Effects of the Mutation of Conserved Acidic Residues on the Spermine Binding and the Conformation of GIRK$_{CP}$—Asp-260 and Asp-275, respectively, exist at the center and the exit on the intracellular side of the pore and lack intersubunit contacts, while Glu-250 and Glu-300 are located at the subunit-subunit interface. To evaluate the contribution of the two acidic residues, Asp-260 and Glu-300, to the spermine binding, the mutants that neutralize their negative charge (D260N and

E300N) were characterized by ITC and NMR. In addition, we investigated two other acidic residues, Glu-250 and Asp-275, using the E250N and D275N mutants.

ITC experiments revealed no heat exchange upon spermine injections to E250N, D260N, or E300N (data not shown). The affinity of D275N for spermine was essentially identical to that of the wild-type protein (Table 2).

The chemical shift differences between these mutants and the wild type were then investigated by ^{1}H-^{15}N TROSY spectra. The Asn mutations of Glu-250 and Glu-300, which are located at the subunit-subunit interface, generated TROSY spectra different from that of the wild type. The spectral overlay between the E300N mutant and the wild type is shown in Fig. 6. Eleven signals were shifted by the E300N mutation to the extent that they are not overlapped with the corresponding signals from the wild type protein: Phe-46, Gly-58, Thr-193, Gly-216, Gln-227, Val-253, E300N, Val-303, Glu-304, Thr-306, and Gly-307 (Fig. 6). These residues are located in the region around Glu-300 to the subunit-subunit interface, and the upper part (membrane side) of the protein including G-loop (residues 303–307). The E250N mutant also showed a large spectral difference (data not shown). Because Glu-250 and Glu-300 are involved in direct contacts between two subunits, the wide distribution of the residues affected by the mutations indicates that the relative orientation of the subunits was altered by these mutations.

On the other hand, the charge-neutralizing mutation of Asp-260, which does not contact any atom of the other subunit, introduced chemical shift changes to the NMR signals from the following residues: Gln-227, Val-253, Thr-257, D260N, and Gln-261 (Fig. 7). The five affected residues are all adjacent to Asp-260, indicating that the effect of the D260N mutation is local effect and does not lead to the relative orientation of the subunits.

The spectral difference of the D275N mutant from the wild type

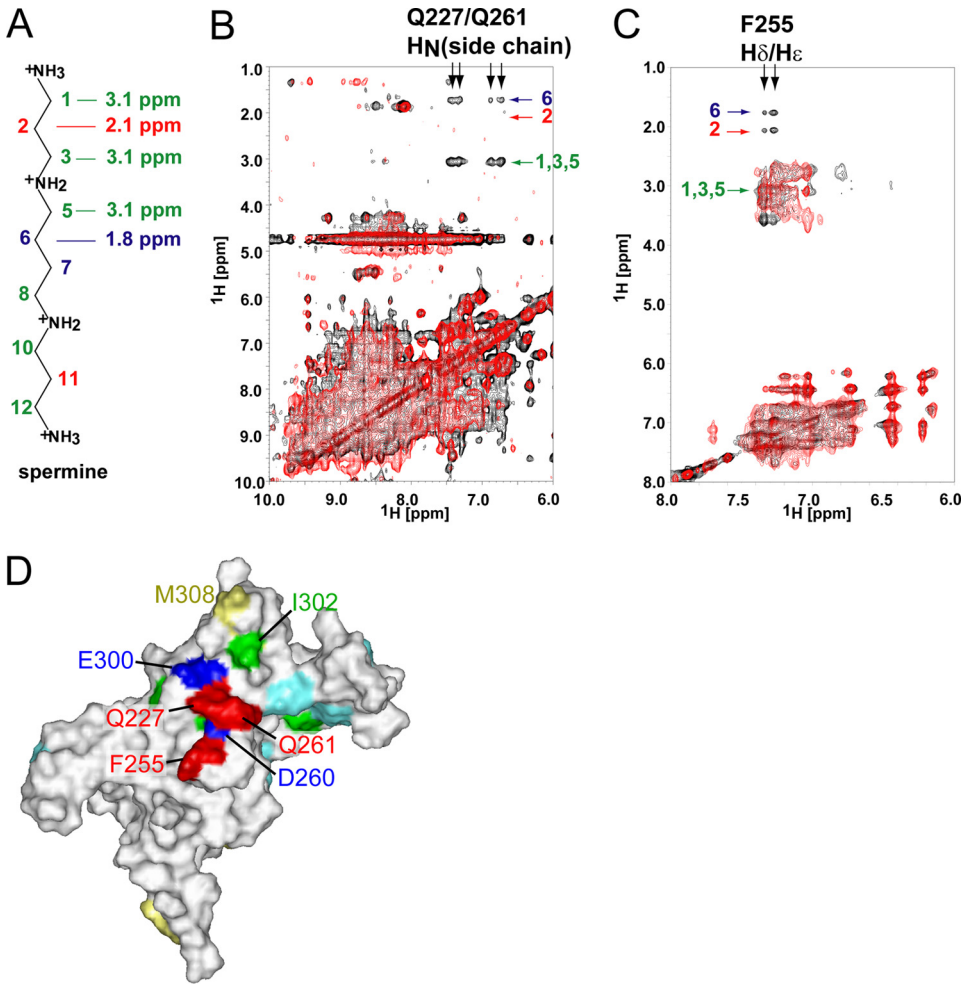

FIGURE 4. **Intermolecular NOE signals between GIRK$_{CP}$ and spermine.** *A*, chemical structure of spermine, labeled the positions of the methylene groups and their chemical shifts. The chemical shift values are shown for positions 1–3 and 5–6, due to the symmetry of the molecule. *B*, overlay of the two-dimensional ^{15}N-edited NOESY HSQC spectra for uniformly ^{2}H,^{15}N-labeled GIRK$_{CP}$ in complex with spermine. The spectra for wild type GIRK-spermine and that for the mutant Q227A/Q261A-spermine are shown in *black* and *red*, respectively. The assignments of the intermolecular NOE signals are indicated. *C*, overlay of the NOESY spectra for phenylalanine-selective ^{1}H,^{15}N-labeled GIRK$_{CP}$ in a ^{2}H-background in complex with spermine. The spectra for wild type GIRK-spermine and that for the mutant F255A-spermine are shown in *black* and *red*, respectively. The assignments of the intermolecular NOE signals are indicated. *D*, mapping of the residues with the intermolecular NOEs. The residues with the intermolecular NOEs, Gln-227, Phe-255, and Gln-261 are mapped in *red* on a surface representation of one of the subunits in the GIRK$_{CP}$ tetramer, which is viewed from the inside of the pore. The amino acid selectively ^{1}H-labeled residues, Ile, Met, and Phe (except for Phe-255), which were used to survey the intermolecular NOE with spermine, are colored *green*, *yellow*, and *cyan*, respectively. The positions of Asp-260 and Glu-300 are also indicated in *blue*.

TABLE 2

Thermodynamic parameters for the interactions of GIRK$_{CP}$ mutants with spermine

Mutant	Model	Stoichiometry per tetramer	K_d	ΔH	ΔS
			μM	*kcal/mol*	*kcal/mol K*
Wild type[a]	Single sites	1.54 ± 0.01	0.82 ± 0.09	−1.93 ± 0.02	0.021
E250N	N/A				
D260N	N/A				
D275N	Single sites	1.74 ± 0.01	1.4 ± 0.1	−2.09 ± 0.02	0.02
E300N	N/A				
Q227A/Q261A	Single sites	1.656 ± 0.003	0.29 ± 0.01	−6.75 ± 0.02	0.0073
F255A	Single sites	1.194 ± 0.005	3.0 ± 0.2	−0.845 ± 0.05	0.022

[a] Data for the wild type GIRK$_{CP}$ are presented for reference.

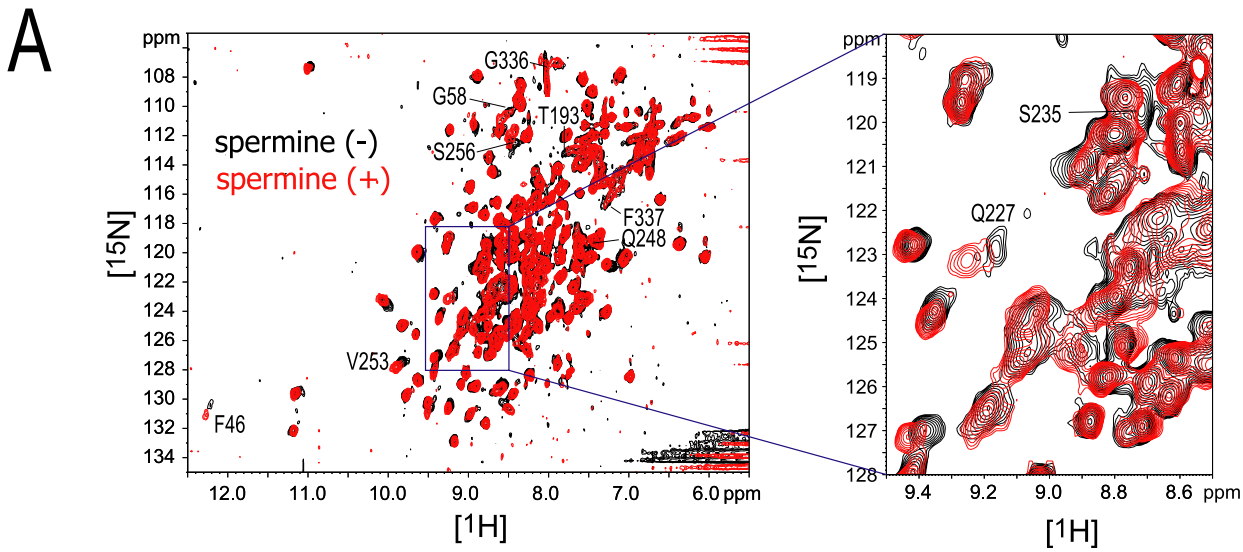
A
ppm
[15N]
[1H]
spermine (-)
spermine (+)
G336
G58
T193
S256
F337
Q248
V253
F46
S235
Q227
12.0
11.0
10.0
9.0
8.0
7.0
6.0 ppm
9.4
9.2
9.0
8.8
8.6 ppm

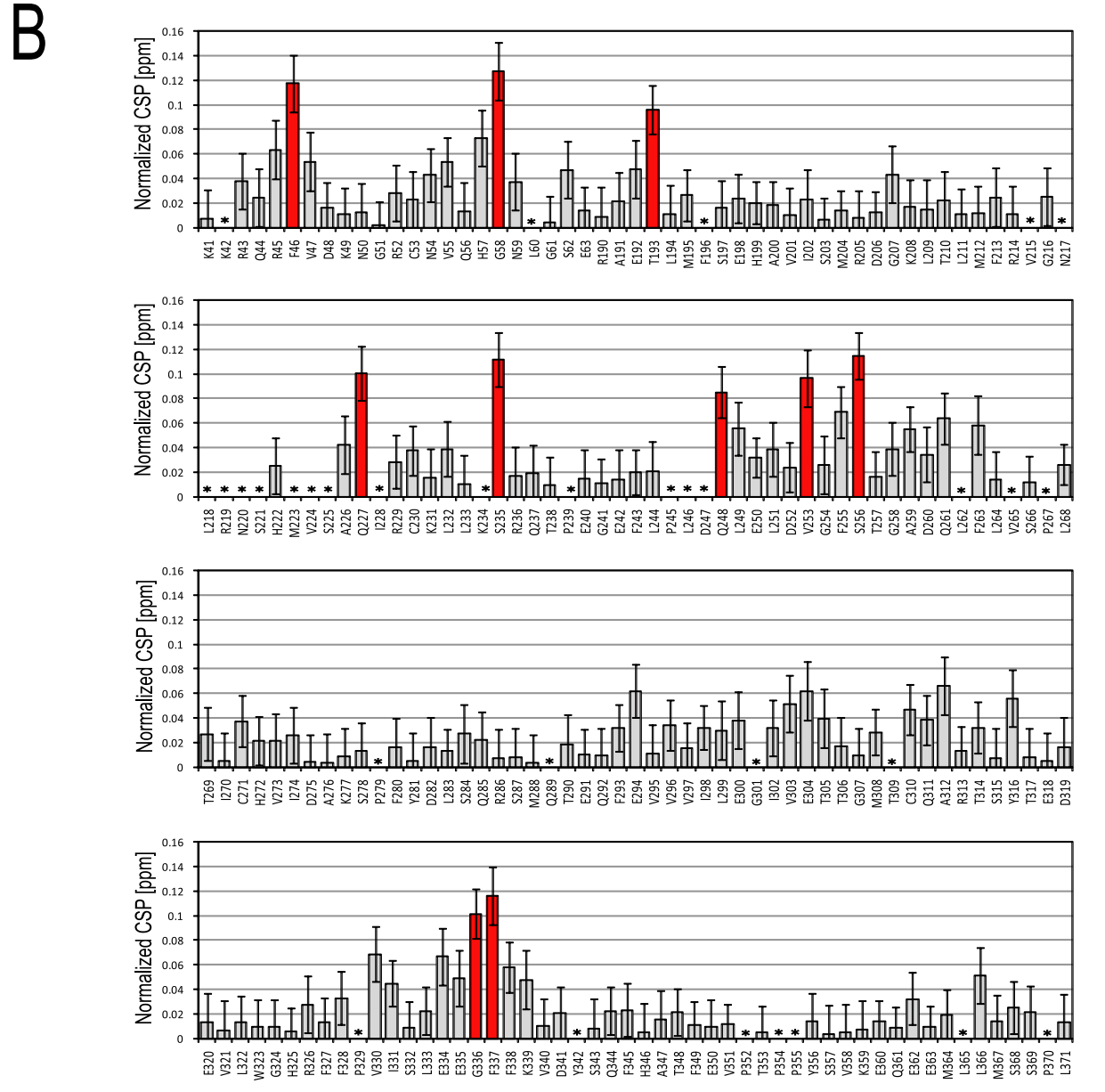
B
Normalized CSP [ppm]
K41 K42 R43 Q44 R45 F46 V47 D48 K49 N50 G51 R52 C53 N54 V55 Q56 H57 G58 N59 L60 G61 S62 E63 R190 A191 E192 T193 L194 M195 F196 S197 E198 H199 A200 V201 I202 S203 M204 R205 D206 G207 K208 L209 T210 L211 M212 F213 R214 V215 G216 N217
L218 R219 N220 S221 H222 M223 V224 S225 A226 Q227 I228 R229 C230 K231 L232 L233 K234 S235 R236 Q237 T238 P239 E240 G241 E242 F243 L244 P245 L246 D247 Q248 L249 E250 L251 D252 V253 G254 F255 S256 T257 G258 A259 D260 Q261 L262 F263 L264 V265 S266 P267 L268
T269 I270 C271 H272 V273 I274 D275 A276 K277 S278 P279 F280 Y281 D282 L283 S284 Q285 R286 S287 M288 Q289 T290 E291 Q292 F293 E294 V295 V296 V297 I298 L299 E300 G301 I302 V303 E304 T305 T306 G307 M308 T309 C310 Q311 A312 R313 T314 S315 Y316 T317 E318 D319
E320 V321 L322 W323 G324 H325 R326 F327 F328 P329 V330 I331 S332 L333 E334 E335 G336 F337 F338 K339 V340 D341 Y342 S343 Q344 F345 H346 A347 T348 F349 E350 V351 P352 T353 P354 P355 Y356 S357 V358 K359 E360 Q361 E362 E363 M364 L365 L366 M367 S368 S369 P370 L371

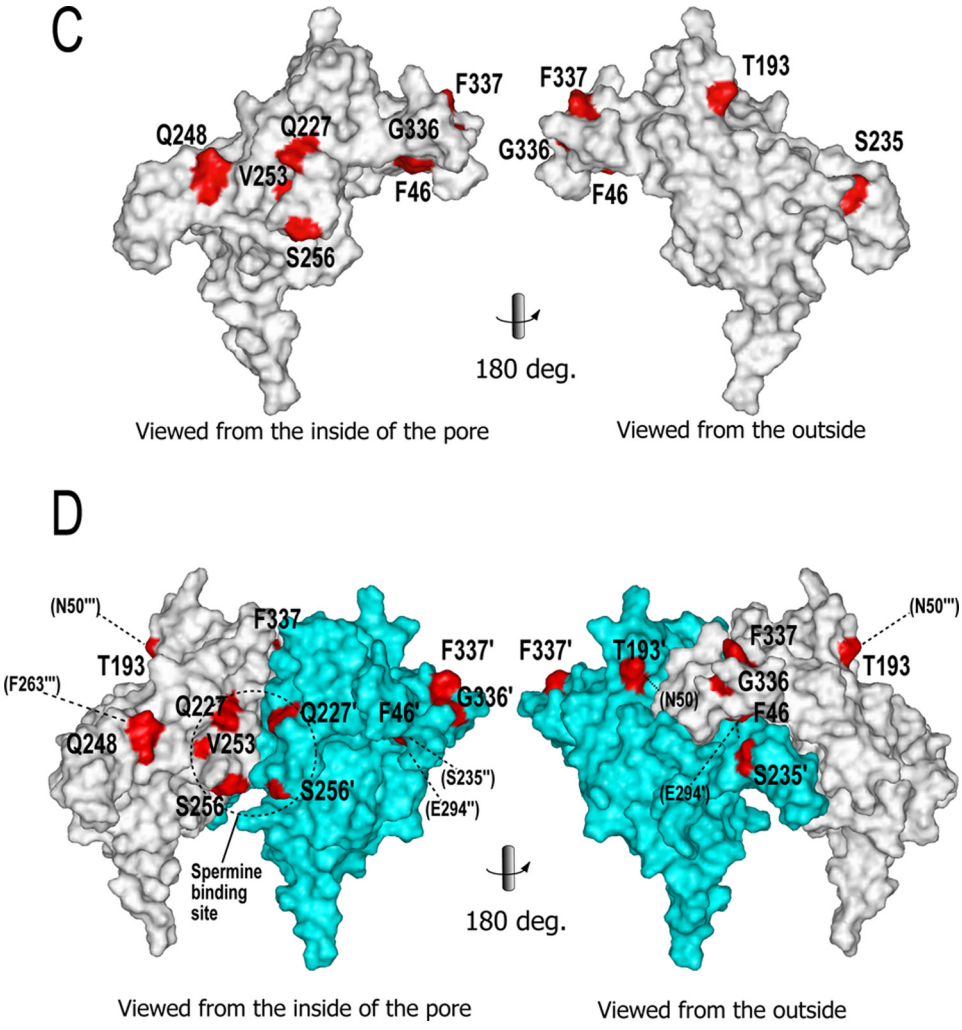

FIGURE 5—*continued*

was limited to Asp-275 and its neighborhood (data not shown). The CSP upon the addition of spermine to D275N was similar to that of the wild type. Considering the result that the spermine binding affinity of D275N is comparable to that of the wild type (Table 2), Asp-275 is involved in neither the direct binding to spermine nor the conformational rearrangement upon spermine binding.

DISCUSSION

Plasticity in the Relative Subunit Orientation of the GIRK$_{CP}$ Tetramer—The ITC results indicated that two spermine molecules bind to a tetramer of GIRK$_{CP}$, with a dissociation constant (K_d) value of 26 μM at the KCl concentration of 150 mM. The KCl concentration dependence of the K_d values (Fig. 2) shows the significant contribution of the electrostatic interaction to the binding between the positive charges of spermine and the negative charges of the acidic residues in GIRK$_{CP}$.

Small but significant CSPs induced by the binding of spermine were observed for the residues at the subunit-subunit interface of the GIRK$_{CP}$ tetramer (Fig. 5). It should be noted that the extent of CSP was relatively small, which might be accounted for by the small structural alteration, or by the averaging of the CSP for the corresponding residues of four subunits of the GIRK$_{CP}$ tetramer. The binding stoichiometry of two molecules of spermine per a tetramer of GIRK$_{CP}$ (Fig. 1 and Table 1) strongly suggests that the tetramer is formed by a dimer of the spermine-bound dimers, producing two distinct types of the subunit-subunit interface: interfaces within and between the spermine-bound dimer. Because the observed CSP is the average of the corresponding residues, which may have different CSPs, in the fast exchange regime on the NMR timescale, it tends to be smaller than the typical CSPs for the conformational change. The residues with the small but significant CSPs distribute widely at the subunit-subunit interfaces, strongly suggesting that spermine binding altered the relative subunit orientation of the tetramer.

The change in the relative orientations of the subunits was also indicated by the NMR spectral differences introduced by the E300N mutation (Fig. 6). Because Glu-300 possesses the contacts with adjacent subunit, the E300N mutation might have caused the subunit rearrangement. These data consistently indicated that GIRK$_{CP}$ possesses the plasticity in the intersubunit orientation of the tetramer.

The plasticity was also suggested by the crystal structures of a Kir3.1-KirBac1.3 chimera, where two channels in the same crystal adopt different conformations through rigid body displacements of the subunits (10). Their relative orientations also

FIGURE 5. **Chemical shift perturbation of the backbone NMR signals of GIRK$_{CP}$ upon spermine binding.** *A*, overlay of the TROSY spectra in the presence (*red*) and absence (*black*) of spermine. The samples contain 100 μM GIRK$_{CP}$ tetramer and 200 μM spermine (*red*), or 137 μM GIRK$_{CP}$ (*black*), respectively. The signals with CSPs larger than 0.08 ppm are labeled. *B*, CSP upon spermine binding. The *x* and *y* axes depict the residues of GIRK$_{CP}$ and the normalized CSP values: $\{(\Delta\delta_{1H})^2 + (\Delta\delta_{15N}/6.5)^2\}^{0.5}$ (25). The CSPs larger than 0.08 ppm are indicated as *red bars*. The error bars were calculated based on the digital resolution. *Asterisks* indicate the residues with no data. *C*, residues with significant CSPs in *B* are colored *red*, with their names on the surface of the single subunit of the crystal structure (PDB code: 1N9P), viewed from the center of the tetramer pore (*left*) and from the outside (*right*). Because the coordinates of Gly-58 are missing in the PDB file, Gly-58 was not able to be mapped on the structure. *D*, mapping of the residues with CSPs (*red*) on the two adjacent subunits in the GIRK$_{CP}$ tetramer (*white* and *cyan*). The residues on the *cyan* and *white* subunits are labeled with and without a prime (′). Adjacent residues in other subunits, which are proximal to the residues with CSPs, are shown in *parentheses* with *dotted lines*, where *double* and *triple primes* indicate the different subunits. The *dotted circle* depicts the spermine binding site.

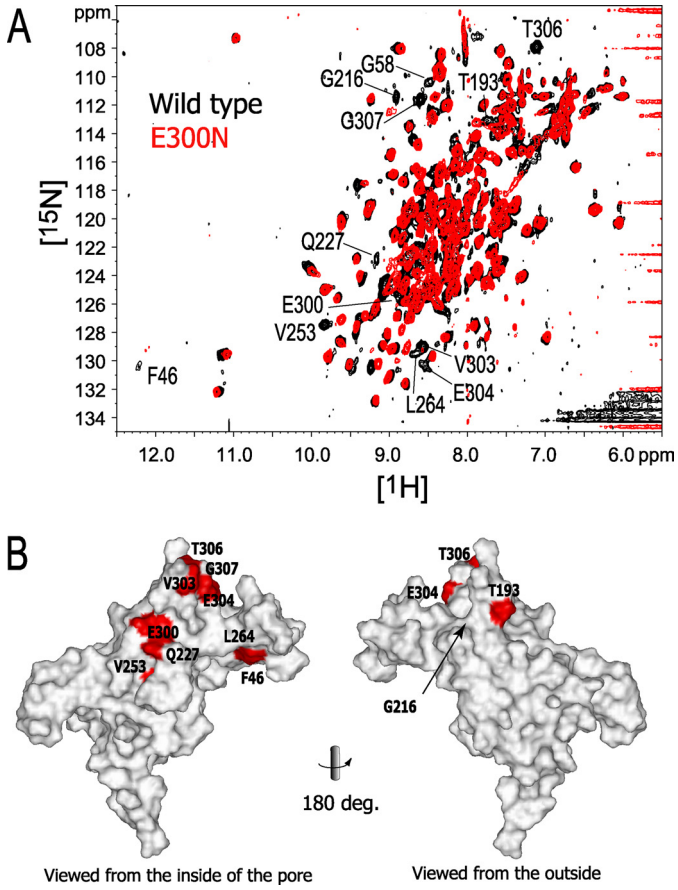

FIGURE 6. **The effect of the E300N mutation on the chemical shift.** *A*, The ^{1}H-^{15}N TROSY signals of the E300N mutant that do not overlap with the corresponding signals from the wild-type protein are labeled. *B*, mapping of the affected residues on the surface of a subunit, viewed from the center of the tetramer pore (*left*) and from the outside (*right*). The buried residue (Gly-216) is indicated with an *arrow*. Because the coordinates of Gly-58 are missing in the PDB file, they were not able to be mapped on the structure.

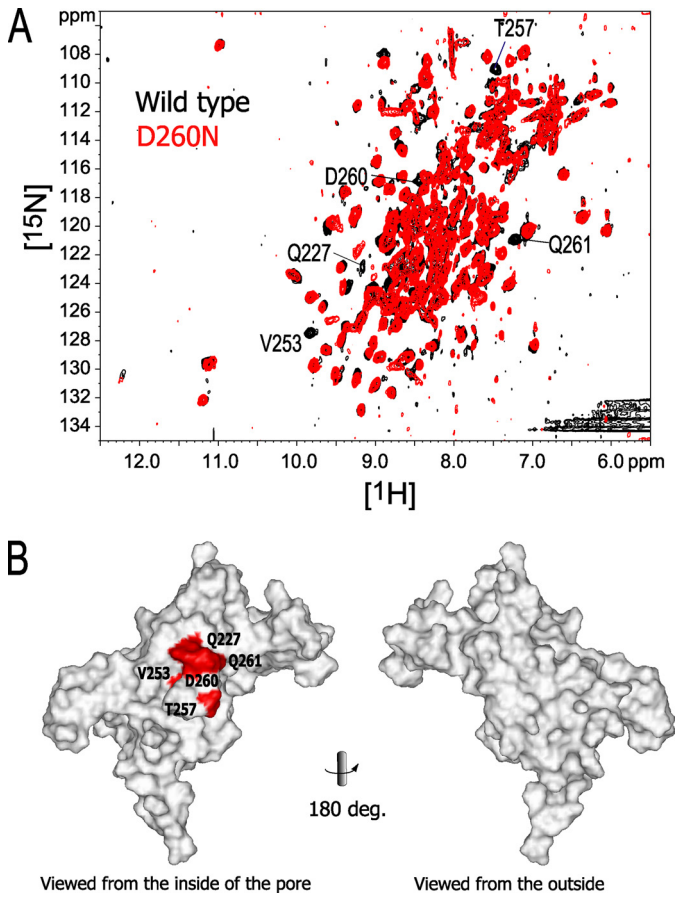

FIGURE 7. **The effect of the D260N mutation on the chemical shift.** *A*, ^{1}H-^{15}N TROSY signals with chemical shift change larger than the signal line width between the wild type and D260N are labeled. *B*, mapping of the affected residues on the surface of a subunit, viewed from the center of the tetramer pore (*left*) and from the outside (*right*). Buried residues are indicated with an *arrow*. Because the coordinates of Gly-58 are missing in the PDB file, Gly-58 was not able to be mapped on the structure.

differ from those in the previous structures of the cytoplasmic pore of Kir3.1/GIRK1 (7, 9). By focusing on Asp-260 in these structures, we noticed that the distances between the oxygen atoms of the Asp-260 carboxyl group from the adjacent subunit range from 9.3 Å (PDB code: 1N9P) to 11.3 Å (PDB code: 2QKS, molecule B).

The Spermine Binding Site on Kir3.1/GIRK1—To date, the results of electrophysiological studies using mutants of Kir2.1 (9, 13, 14) have suggested that the intracellular acidic residues in Kir3.1, Asp-260 and Glu-300, are critical residues for the inward rectification. Our ITC results also indicated that D260N and E300N do not bind to spermine. However, our NMR data consistently support that Asp-260, not Glu-300, interacts directly with spermine: (1) Intermolecular transferred NOE signals were observed for Gln-227, Gln-261, and Phe-255, which surround Asp-260 (Fig. 4), while no NOE signals with spermine were observed for the Ile or Met side chains, which are located in the proximity of Glu-300 (2). CSPs upon the addition of spermine were not observed for the site around Glu-300, but were found for the residues surrounding Asp-260 (Fig. 5*D*) (3). While the residues with remarkable chemical shift changes by the D260N mutation is limited to the proximity (Fig. 7), those by the E300N mutation are distributed widely at the subunit-subunit interface of the tetramer (Fig. 6). Therefore, the impaired spermine affinity of the E300N mutant might be due to the structural rearrangement of the four subunits.

Based on these results, we conclude that Asp-260, not Glu-300, is the negatively charged residue that is critical for the direct binding of spermine. This is also consistent with the recent electrostatics calculation report, indicating that Asp-260 is the strongest negatively charged contributor to the electrostatics of the cytoplasmic regions of Kir3.1 (26).

The aspartate residue corresponding to Asp-260 in Kir3.1/GIRK1 is highly conserved in other human Kirs except for Kir6; Kir2.1–2.4, 3.1–3.4, and 4.1, and is substituted by another acidic residue, glutamate, in Kir1.1 and 1.3 and 7.1. Therefore, the binding site identified here in Kir3.1/GIRK1 might exist in other Kirs. However, the numbers and positions of the acidic residues in the cytoplasmic pore differ among the Kirs, suggesting that alternative binding sites might be found in other Kirs.

The Spermine Binding Mode—We have proposed the spermine binding mode to Kir3.1/GIRK1, based on the pattern of the intermolecular transferred NOEs, the binding stoichiometry, and the electrostatic interaction with Asp-260 (Fig. 8). It should be noted that the protein structure used for the schematic illustration in Fig. 8 represents the spermine-free state, which is different from the spermine-

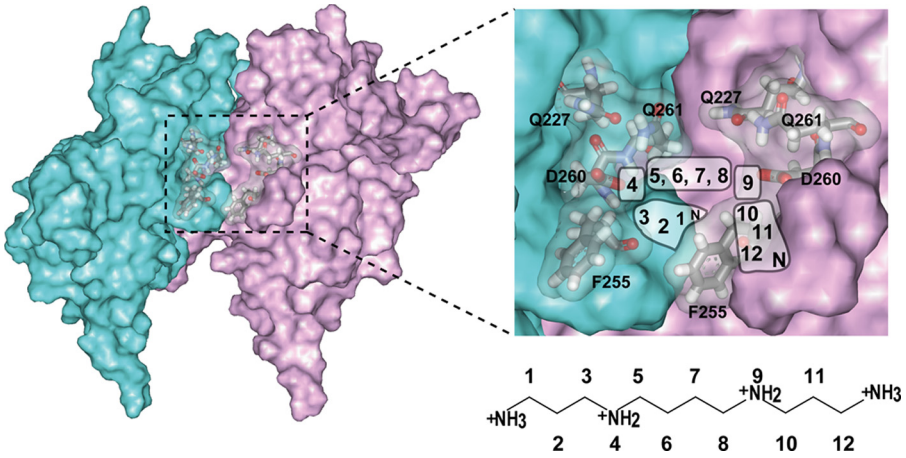

FIGURE 8. **The postulated spermine binding mode.** Two adjacent subunits of the tetramer of $GIRK_{CP}$ are shown as the surfaces colored *cyan* and *magenta*, in which the spermine binding site is indicated by the *dotted rectangle* (*left*). The postulated areas for the spermine atoms in the binding site are illustrated (*right*). The residues identified in this study are labeled.

bound state. While all of the proton sites of spermine exhibited NOEs with the aromatic protons of Phe-255, only positions 5 and 6 of the spermine protons showed NOEs with the side chain amide protons of Gln-227 and Gln-261 (Fig. 4). Because the NOE signals from position 2 of spermine were observed only with Phe-255, and not with Gln-227/Gln-261, both termini of the spermine should be close to Phe-255 and away from Gln-227/Gln-261, while the central methylene groups at positions 5 and 6 (and the symmetrical positions 7 and 8) should point upward toward Gln-227/Gln-261. Because Asp-260 exists between Phe-255 and Gln-227/Gln-261, the positive charges on the nitrogen atoms of spermine at positions 4 and 9 interact with the negative charge of the Asp-260 side chain. The spermine binding stoichiometry of two per tetramer of $GIRK_{CP}$, suggests that one spermine molecule bridges the two negative charges of the Asp-260 residues of adjacent subunits in the GIRK tetramer.

The Role of Spermine Binding to the Cytoplasmic Pore—As shown in Fig. 5, spermine binding changed the chemical shifts of the residues at the subunit-subunit interface, in addition to those of the direct binding site. This seems to be related to the spermine binding mode; a molecule of spermine bridges two Asp-260 side chains, stabilizing a certain orientation of the four subunits of the tetramer.

Kir3/GIRK is activated by the binding of G-protein $\beta\gamma$ subunits ($G\beta\gamma$) to the intracellular regions. FRET microscopy indicated that the intracellular regions of the GIRK1/GIRK4 channel exhibit conformational rearrangements upon $G\beta\gamma$ binding (22). Our data revealed that spermine binding stabilizes a certain intersubunit orientation, which is probably different from that of the $G\beta\gamma$-bound state. Therefore, the spermine binding to the cytoplasmic pore might contribute to the stabilization of the resting state of the channel.

Conversely, the $G\beta\gamma$-induced rearrangement of the four subunits of Kir3.1/GIRK1 upon its activation could disrupt the ability of spermine to bridge the two Asp-260 side chains, leading to impaired affinity for spermine. Therefore, the spermine binding mode revealed here suggests that spermine is dissociated from the cytoplasmic pore of the channel upon its activation. Because the spermine binding site is at the center of the cytoplasmic pore, the dissociation from the site would be beneficial for the access to the final binding site in the transmembrane region, to accomplish the blockade of the outward K^+ current.

Conclusion—We have described here the affinity, stoichiometry, sites, and mode of spermine binding to the intracellular regions of Kir3.1/GIRK1. The direct binding site of spermine on the Kir channel was first identified, based on the distance information of the intermolecular NOEs. Importantly, spermine bridges two Asp-260 side chains, inducing a change in the relative orientations of the four subunits of the tetramer. Thus, spermine could be dissociated from the cytoplasmic pore upon channel activation by the $G\beta\gamma$-induced conformational rearrangement. Spermine exerts the voltage-dependent blockade of the outward current, presumably in the transmembrane pore. The activation-dependent dissociation of spermine from the cytoplasmic pore seems to play a role in the rapid and efficient blockade of the transmembrane pore.

REFERENCES

1. Bichet, D., Haass, F. A., and Jan, L. Y. (2003) *Nat. Rev. Neurosci.* **4,** 957–967
2. Ficker, E., Taglialatela, M., Wible, B. A., Henley, C. M., and Brown, A. M. (1994) *Science* **266,** 1068–1072
3. Lopatin, A. N., Makhina, E. N., and Nichols, C. G. (1994) *Nature* **372,** 366–369
4. Lopatin, A. N., Makhina, E. N., and Nichols, C. G. (1995) *J. Gen. Physiol.* **106,** 923–955
5. Fakler, B., Brändle, U., Glowatzki, E., Weidemann, S., Zenner, H. P., and Ruppersberg, J. P. (1995) *Cell* **80,** 149–154
6. Stanfield, P. R., Nakajima, S., and Nakajima, Y. (2002) *Rev. Physiol. Biochem. Pharmacol.* **145,** 47–179
7. Nishida, M., and MacKinnon, R. (2002) *Cell* **111,** 957–965
8. Kuo, A., Gulbis, J. M., Antcliff, J. F., Rahman, T., Lowe, E. D., Zimmer, J., Cuthbertson, J., Ashcroft, F. M., Ezaki, T., and Doyle, D. A. (2003) *Science* **300,** 1922–1926
9. Pegan, S., Arrabit, C., Zhou, W., Kwiatkowski, W., Collins, A., Slesinger, P. A., and Choe, S. (2005) *Nat. Neurosci.* **8,** 279–287
10. Nishida, M., Cadene, M., Chait, B. T., and MacKinnon, R. (2007) *EMBO J.* **26,** 4005–4015
11. Lu, Z., and MacKinnon, R. (1994) *Nature* **371,** 243–246
12. Stanfield, P. R., Davies, N. W., Shelton, P. A., Sutcliffe, M. J., Khan, I. A., Brammar, W. J., and Conley, E. C. (1994) *J. Physiol.* **478,** 1–6
13. Yang, J., Jan, Y. N., and Jan, L. Y. (1995) *Neuron* **14,** 1047–1054
14. Kubo, Y., and Murata, Y. (2001) *J. Physiol.* **531,** 645–660
15. Xie, L. H., John, S. A., and Weiss, J. N. (2003) *J. Physiol.* **550,** 67–82
16. Guo, D., and Lu, Z. (2003) *J. Gen. Physiol.* **122,** 485–500
17. Guo, D., Ramu, Y., Klem, A. M., and Lu, Z. (2003) *J. Gen. Physiol.* **121,** 261–275
18. Fujiwara, Y., and Kubo, Y. (2006) *J. Gen. Physiol.* **127,** 401–419
19. Kurata, H. T., Cheng, W. W., Arrabit, C., Slesinger, P. A., and Nichols, C. G. (2007) *J. Gen. Physiol.* **130,** 145–155
20. Frassineti, C., Alderighi, L., Gans, P., Sabatini, A., Vacca, A., and Ghelli, S. (2003) *Anal. Bioanal. Chem.* **376,** 1041–1052
21. Kurata, H. T., Phillips, L. R., Rose, T., Loussouarn, G., Herlitze, S., Fritzen-

schaft, H., Enkvetchakul, D., Nichols, C. G., and Baukrowitz, T. (2004) *J. Gen. Physiol.* **124,** 541–554
22. Riven, I., Kalmanzon, E., Segev, L., and Reuveny, E. (2003) *Neuron* **38,** 225–235
23. Yokogawa, M., Muramatsu, T., Takeuchi, K., Osawa, M., and Shimada, I. (2009) *Biomol. NMR Assign.* **3,** 125–128
24. Wiseman, T., Williston, S., Brandts, J. F., and Lin, L. N. (1989) *Anal. Biochem.* **179,** 131–137
25. Mulder, F. A., Schipper, D., Bott, R., and Boelens, R. (1999) *J. Mol. Biol.* **292,** 111–123
26. Robertson, J. L., Palmer, L. G., and Roux, B. (2008) *J. Gen. Physiol.* **132,** 613–632